

# Enhancing the Magnetic and Magneto-optical Properties of Praseodymium-substituted Bi-YIG Thin Film on Glass Substrate Prepared by Metal-organic Decomposition

Viet Dongquoc<sup>1†</sup>, Trinh Nguyen Thi<sup>1†</sup>, Phuoc Cao Van<sup>1</sup>, Duc Duong Viet<sup>1</sup>,  
Ha-Young Ahn<sup>1</sup>, Eui-Tae Kim<sup>1</sup>, Seung-Young Park<sup>2\*</sup>, and Jong-Ryul Jeong<sup>1\*</sup>

<sup>1</sup>Department of Materials Science and Engineering, Chungnam National University, Daejeon 34134, Republic of Korea

<sup>2</sup>Center for Scientific Instrumentation, Korea Basic Science Institute, Daejeon 34133, Republic of Korea

(Received 6 January 2021, Received in final form 10 March 2021, Accepted 10 March 2021)

Praseodymium (Pr)- and bismuth (Bi)-substituted yttrium (Y) iron (Fe) garnet ( $\text{Pr}_x\text{Y}_{2-x}\text{Bi}_1\text{Fe}_5\text{O}_{12}$  where  $x = 0.25, 0.5, 1,$  and  $2$ ) thin films were prepared on glass substrate using a metal-organic decomposition (MOD) method. Their magneto-optical properties were studied as a function of Pr concentration. Praseodymium has two functions in  $\text{Pr}_x\text{Y}_{2-x}\text{Bi}_1\text{Fe}_5\text{O}_{12}$  thin films, i.e., it (i) improves spin-orbit interaction strength and (ii) increases magnetic properties; both are expected to strongly enhance the Faraday rotation (FR) angle of the thin film. Our study demonstrated that the  $\text{Pr}_1\text{Y}_1\text{Bi}_1\text{Fe}_5\text{O}_{12}$  thin-film displayed the highest FR angle, of  $-13^\circ/\mu\text{m}$ , which is 1.6-times higher than that of the  $\text{Pr}_x\text{Y}_{2-x}\text{Bi}_1\text{Fe}_5\text{O}_{12}$  thin film without Pr dopant. The  $\text{Pr}_1\text{Bi}_1\text{Y}_1\text{Fe}_5\text{O}_{12}$  thin film fabricated on a glass substrate by the MOD method displayed excellent MO performance and is a potential candidate for application in optical devices.

**Keywords** : Bi-YIG thin films, Faraday rotation, magneto-optical properties, metal-organic decomposition, polyvinylpyrrolidone

## 1. Introduction

Although magneto-optical (MO) effects have been known for at least 175 years, they have only recently been applied practically, and the majority of the applications only appeared in the three last decades. The most common applications are spintronics, information storage devices, optical isolators, and optical sensors [1-4]. Notably, MO microscopy is widely used due to its numerous advantages, including a wide operating temperature range, easy experimental setup, and fast processing that can realize real-time imaging of magnetic fields at a spatial resolution of about  $0.6 \mu\text{m}$  [5]. Indicator films in MO microscopy should have a large Faraday rotation (FR) angle, low optical absorption at a given optical limit, and a thin structure. These properties directly influence the sensitivity,

resolution, and quality of MO images [6]. Rare-earth or bismuth (Bi)-substituted yttrium (Y)-iron (Fe)-garnet (YIG) meets all of these requirements. Several methods can be used to prepare garnet thin films, such as liquid-phase epitaxy [7], magnetron sputtering [8, 9], pulsed laser deposition [10], the sol-gel method [11], and metal-organic decomposition (MOD) [12-14]. Among these methods, the MOD method was chosen for this study because of its many advantages including simplicity, low cost, ability to form uniform films of high purity, and good chemical stability [15]. Normally, high-quality garnet films are fabricated on a garnet substrate, because morphological instability due to misfit stress is avoided by using lattice-matched substrates [6]. However, a glass substrate for film deposition is necessary for film quality, especially for large-scale fabrication [16]. Our group has made high-quality Bi-substituted YIG (Bi-YIG) thin films on a glass substrate by using the MOD method and an optimized concentration of polyvinylpyrrolidone (PVP) in a precursor solution containing a metal nitrate [14].

Most previous studies have focused on enhancing the FR angle of Bi-YIG films because this effect is unambiguously associated with the presence of the dia-

©The Korean Magnetism Society. All rights reserved.

\*Corresponding author: Tel: +82-42-821-6633

Fax: +82-42-822-5850, e-mail: jrjeong@cnu.ac.kr

Tel: +82-42-865-3655, Fax: +82-42-865-3499

e-mail: syark@kbsi.re.kr

†These authors contributed equally to this work.

magnetic  $\text{Bi}^{3+}$  ion, which has a large spin-orbit coupling constant. The behavior has also been attributed to increased spin-orbit coupling of  $\text{Fe}^{3+}$  ions resulting from a molecular orbital, formed by mixing the 3d  $\text{Fe}^{3+}$  orbital with the 6p  $\text{Bi}^{3+}$  orbital via 2p orbitals of  $\text{O}^{2-}$  ions [17-19]. The large spin-orbit coupling induces a large excited-state splitting that enhances the FR angle [20].

In addition to the well-known  $\text{Bi}^{3+}$  ion, light rare-earth ions, such as  $\text{Ce}^{3+}$ ,  $\text{Pr}^{3+}$ , and  $\text{Nd}^{3+}$  ions that have radii close to that of  $\text{Bi}^{3+}$ , also strongly enhance MO activity in Fe garnets in the visible and near-infrared regions [21]. Many studies have reported that praseodymium (Pr)-substituted YIG can be used to boost the magnetic and MO properties of the garnet film. For example, Yang *et al.* reported a strong influence of the spin-orbit coupling strength of the ground configuration on the FR angle of Pr-substituted YIG [22]. Hansen *et al.* fabricated a garnet film of composition  $\text{Y}_{3-x-y}\text{Pr}_x\text{Bi}_y\text{Fe}_5\text{O}_{12}$ , and reported that the  $\text{Pr}^{3+}$  ions induced a negative, and the  $\text{Bi}^{3+}$  ions a positive, uniaxial anisotropy. Moreover, both ions strongly affected the saturation magnetization ( $M_S$ ) and FR angle [23]. Akhtar *et al.* prepared multiple rare-earth metal cations (Gd, Yb, Ho, and Pr)-doped YIG films and found that  $\text{Y}_{2.8}\text{Pr}_{0.2}\text{Fe}_5\text{O}_{12}$  had a significantly enhanced  $M_S$  [24]. However, the effect of Pr concentration in the garnet thin film made by the MOD method has not been investigated.

Herein, we prepared garnet films of various compositions ( $\text{Pr}_x\text{Y}_{2-x}\text{Bi}_1\text{Fe}_5\text{O}_{12}$ , where  $x = 0.25, 0.5, 1, \text{ and } 2$ ) on a glass substrate by modifying the MOD method. The effects of changing the composition on magnetic and MO properties were studied. The  $\text{Pr}_1\text{Y}_1\text{Bi}_1\text{Fe}_5\text{O}_{12}$  thin-film displayed a very high FR angle of  $-13^\circ/\mu\text{m}$ , which was 1.6-times higher than that of the  $\text{Y}_2\text{Bi}_1\text{Fe}_5\text{O}_{12}$  thin film without Pr dopant.

## 2. Experimental

Figure 1 schematically illustrates the MOD process. The MOD precursor solution consisted of praseodymium nitrate [ $\text{Pr}(\text{NO}_3)_3 \cdot 6\text{H}_2\text{O}$ ], bismuth nitrate [ $\text{Bi}(\text{NO}_3)_3 \cdot 5\text{H}_2\text{O}$ ], yttrium nitrate [ $\text{Y}(\text{NO}_3)_3 \cdot 6\text{H}_2\text{O}$ ], and ferric nitrate [ $\text{Fe}(\text{NO}_3)_3 \cdot 9\text{H}_2\text{O}$ ] (all 99.9 % purity; Sigma–Aldrich, St. Louis, MO, USA). The precursor solution having the desired chemical composition for  $\text{Pr}_x\text{Y}_{2-x}\text{Bi}_1\text{Fe}_5\text{O}_{12}$  ( $x = 0, 0.25, 0.5, 1, \text{ and } 2$ ) was dissolved in dimethylformamide (DMF) with the previously reported optimal amount of PVP [14]. The total metal precursor concentration was fixed at 20 % for all MOD solutions. Thin films were fabricated on a glass substrate using the modified MOD method, as previously reported [13]. In brief, the MOD precursor solution was spin-coated onto glass substrate at 500 rpm for 5 s and 3,000 rpm for 30 s. Then the solvent was evaporated from the film by heating at 100 °C for 30 min on a hot plate. The film was annealed in a tube furnace at 750 °C for 1 h under an oxygen atmosphere. The process was repeated to obtain the desired thickness (~120 nm).

Crystalline and magnetic properties were evaluated by X-ray diffraction (XRD; Bruker D8; Bruker Corp., Billerica, MA, USA) and vibrating sample magnetometry (VSM; 7304; Lake Shore Cryotronics, Inc., Westerville, OH, USA), respectively. Scanning electron microscopy (SEM; S-4800; Hitachi, Ltd., Tokyo, Japan) was used to examine the morphology and thickness of a thin film. The FR measurement was described in our previous report [25]. An HL-2000 system (Ocean Optics, Inc., Largo, FL, USA; wavelength range: 360-2,400 nm) was used as the light source for the measurements.

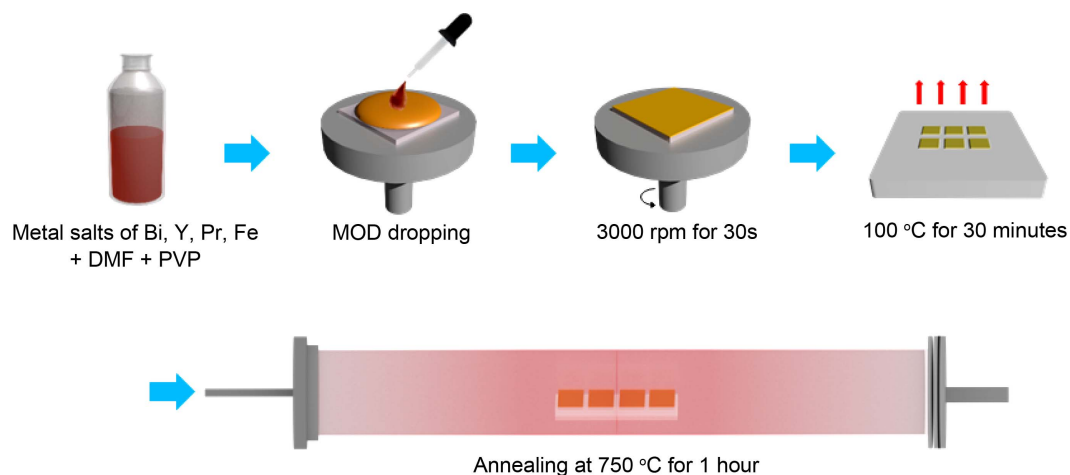


**Fig. 1.** (Color online) Schematic illustration of the metal-organic decomposition (MOD) procedure.

### 3. Results and Discussion

Figure 2(a) presents the FR spectra for the wavelength range of 430-900 nm for  $\text{Pr}_x\text{Y}_{2-x}\text{Bi}_1\text{Fe}_5\text{O}_{12}$  ( $x = 0, 0.25, 0.5, 1,$  and  $2$ ) thin films on glass substrate. The maximum FR angle ( $\theta_{\text{max}}$ ) was strongly dependent on Pr content (Fig. 2(b)). At wavelength 510 nm, the  $\theta_{\text{max}}$  slowly increased with increasing Pr content and reached the highest FR angle of about  $-13^\circ/\mu\text{m}$  with high transmittance of 40 % at a Pr content of  $x = 1$ . For comparison, Bi-YIG without Pr dopant had a  $\theta_{\text{max}}$  of about  $-8^\circ/\mu\text{m}$ . The enhancement of the FR angle was due to two effects: (1) Pr substitution into  $\text{Pr}_x\text{Y}_{2-x}\text{Bi}_1\text{Fe}_5$  increases spin-orbit coupling strength, which strongly influences MO properties [22, 23], and (2) Pr strongly affects the crystalline and magnetic properties of garnet thin films. These effects were investigated by XRD, SEM, and VSM. However, the  $\theta_{\text{max}}$  abruptly decreased to  $-1.6^\circ/\mu\text{m}$  at the highest Pr content ( $x = 2$ ). Faraday hysteresis loops of the  $\text{Pr}_1\text{Bi}_1\text{Y}_1\text{Fe}_5\text{O}_{12}$  film measured at 455 and 510 nm are presented in Fig. 2(c) and (d), respectively. In Fig. 2(c), the shape of the hysteresis loop displays a positive FR and a maximum value of  $4.5^\circ/\mu\text{m}$ , while a negative FR with a maximum value of  $-13^\circ/\mu\text{m}$  is shown in Fig. 2(d).

To elucidate the enhancement of  $\theta_{\text{max}}$  in  $\text{Pr}_x\text{Y}_{2-x}\text{Bi}_1\text{Fe}_5\text{O}_{12}$  thin films, we first investigated the crystallinity of the

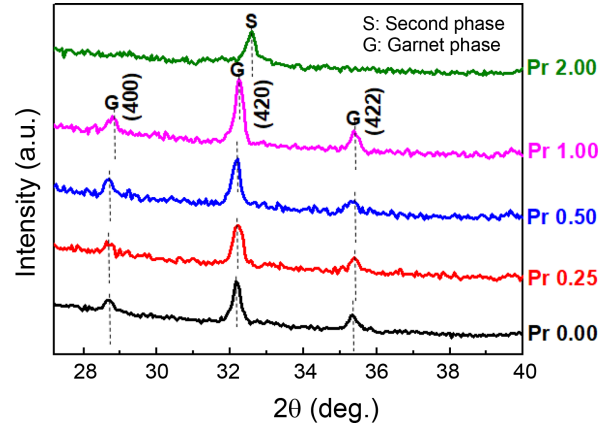


**Fig. 3.** (Color online) X-ray diffraction patterns of  $\text{Pr}_x\text{Y}_{2-x}\text{Bi}_1\text{Fe}_5\text{O}_{12}$  thin films on a glass substrate as a function of Pr content.

films. Figure 3 shows the XRD pattern of the  $\text{Pr}_x\text{Y}_{2-x}\text{Bi}_1\text{Fe}_5\text{O}_{12}$  thin films with  $x = 0, 0.25, 0.5, 1,$  and  $2$ . Thin films having lower Pr contents ( $x = 0, 0.25, 0.5,$  and  $1$ ) displayed the garnet phase only. The YIG peaks corresponded to the (400), (420), and (422) planes, with the strongest peak seen at  $2\theta = 32^\circ$  for the (420) plane. The  $\text{Pr}_1\text{Y}_1\text{Bi}_1\text{Fe}_5$  thin-film displayed the most intense garnet-phase peak. In addition, the relative intensities of the (420)/(400) and (420)/(422) peaks of the  $\text{Pr}_1\text{Y}_1\text{Bi}_1\text{Fe}_5$  thin film were higher than those of the other thin films. The

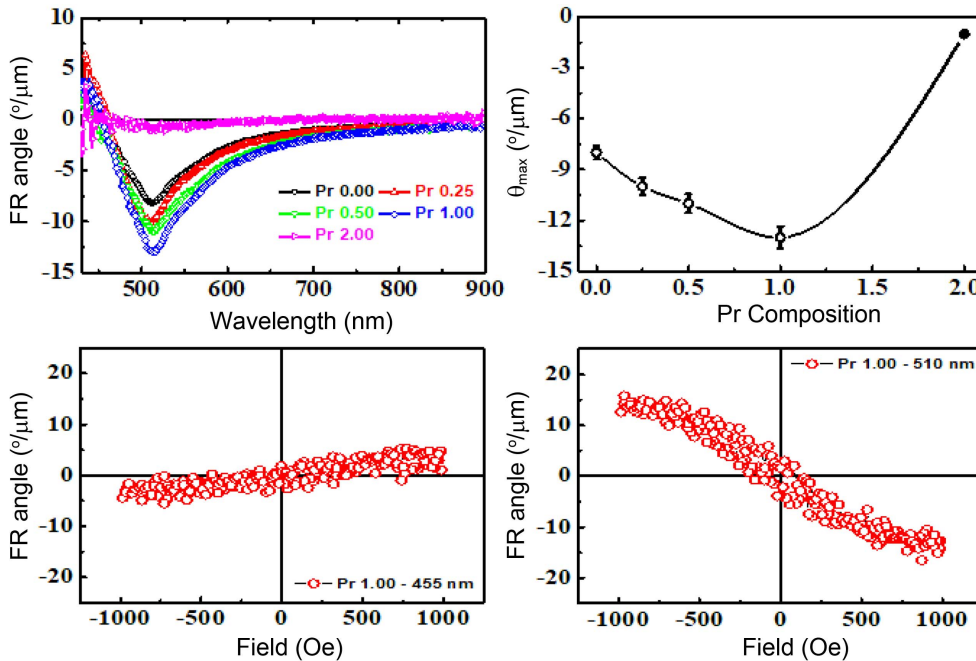


**Fig. 2.** (Color online) (a) Faraday rotation (FR) spectra of  $\text{Pr}_x\text{Y}_{2-x}\text{Bi}_1\text{Fe}_5\text{O}_{12}$  ( $x = 0.25, 0.5, 1,$  and  $2$ ) as a function of praseodymium (Pr) content. (b) Maximum FR angle ( $\theta_{\text{max}}$ ) as a function of Pr content. (c)-(d) Faraday hysteresis loops of the  $\text{Pr}_1\text{Bi}_1\text{Y}_1\text{Fe}_5\text{O}_{12}$  film at 455 and 510 nm, respectively.

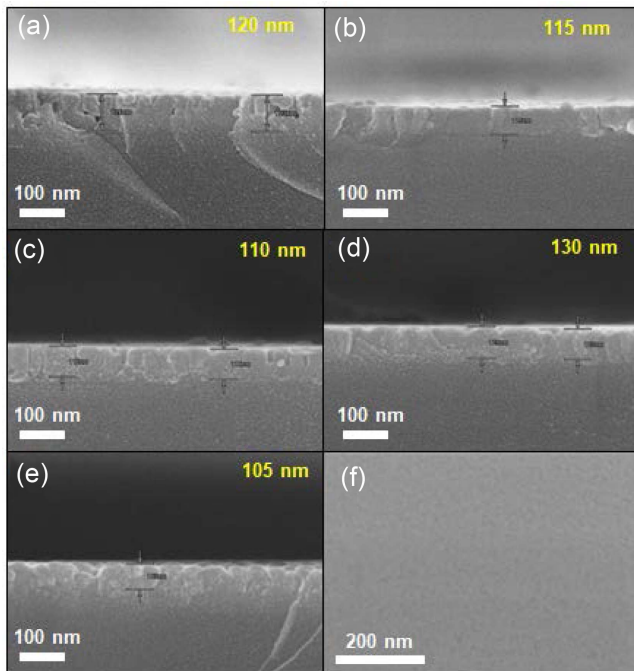


**Fig. 4.** (Color online) Cross-sectional scanning electron microscopy images of (a) Bi-YIG and  $\text{Pr}_x\text{Y}_{2-x}\text{Bi}_1\text{Fe}_5\text{O}_{12}/\text{glass}$  as a function of Pr content for  $x =$  (b) 0.25, (c) 0.5, (d) 1, and (e) 2. (f) Surface morphology of the  $\text{Pr}_1\text{Bi}_1\text{Y}_1\text{Fe}_5\text{O}_{12}$  film.

XRD results proved that the  $\text{Pr}_1\text{Y}_1\text{Bi}_1\text{Fe}_5\text{O}_{12}$  thin film on glass had higher crystallinity compared with the other films. However, the XRD pattern of the  $\text{Pr}_2\text{Bi}_1\text{Fe}_5\text{O}_{12}$  film displayed a second phase with low crystallinity at  $2\theta = 32.54^\circ$ .

Figure 4(a)-(e) presents cross-sectional SEM images of  $\text{Pr}_x\text{Y}_{2-x}\text{Bi}_1\text{Fe}_5\text{O}_{12}$  ( $x = 0, 0.25, 0.5, 1,$  and  $2$ ) on glass substrate. At lower Pr contents ( $x = 0, 0.25, 0.5,$  and  $1$ ), the thin films grew on the glass substrate with good uniformity, high densification and less pores. The thickness of the thin films was uniform over the range of 120-130 nm (Fig. 4(a)-(d)). However, at the highest Pr content ( $x = 2$ ), the thin film thickness was not uniform and the film had a rough skin (Fig. 4(e)). These results are in good agreement with the XRD results shown in Fig. 3. The SEM surface images of the  $\text{Pr}_1\text{Y}_2\text{Bi}_1\text{Fe}_5\text{O}_{12}$  thin films presented in Fig. 4(f) reveal an absence of pores and cracks and a smooth surface.

Figure 5(a)-(e) presents the magnetization hysteresis loops for  $\text{Pr}_x\text{Y}_{2-x}\text{Bi}_1\text{Fe}_5\text{O}_{12}$  ( $x = 0, 0.25, 0.5, 1,$  and  $2$ ), for in- and out-of-plane magnetic fields. For the in-plane magnetic field, the magnetization of the  $\text{Pr}_x\text{Y}_{2-x}\text{Bi}_1\text{Fe}_5\text{O}_{12}$  thin films reached saturation at a lower magnetic field

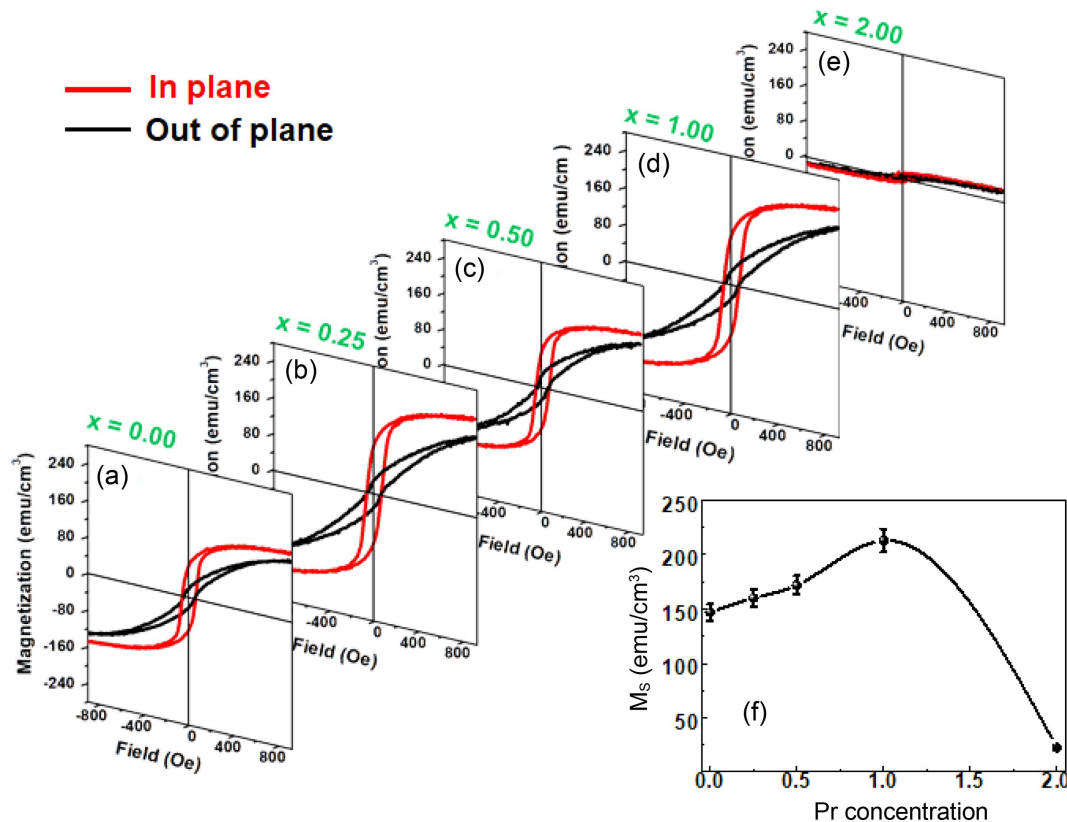


**Fig. 5.** (Color online) (a)-(e) In- and out-of-plane magnetization hysteresis loops of  $\text{Pr}_x\text{Y}_{2-x}\text{Bi}_1\text{Fe}_5\text{O}_{12}/\text{glass}$  for  $x = 0, 0.25, 0.5, 1.5,$  and  $2$ . (f) Variation in the saturation magnetization of the  $\text{Pr}_x\text{Y}_{2-x}\text{Bi}_1\text{Fe}_5\text{O}_{12}$  thin film as a function of Pr content.

strength of 150 Oe, while the out-of-plane magnetic hysteresis loops were not saturated. This proved that the  $\text{Pr}_x\text{Y}_{2-x}\text{Bi}_1\text{Fe}_5\text{O}_{12}$  thin film made by the MOD method on glass substrate had a magnetic anisotropy parallel to the film plane, which is vital for application as a MO-microscopy indicator film [12]. The  $M_S$  values (in-plane) as a function of  $\text{Pr}_x\text{Y}_{2-x}\text{Bi}_1\text{Fe}_5\text{O}_{12}$  ( $x = 0, 0.25, 0.5, 1,$  and  $2$ ) are presented in Fig. 5(f). The  $M_S$  values correspond to the sample crystallinities and morphologies shown in Figs. 3 and 4, respectively. In detail, the  $M_S$  improved with increasing Pr content and reached a maximum of  $200 \text{ emu/cm}^3$  for  $\text{Pr}_1\text{Y}_1\text{Bi}_1\text{Fe}_5\text{O}_{12}$ . The  $M_S$  enhancement was attributed to the doping of  $\text{Pr}^{3+}$  in garnet phase structure, which changes the tetrahedral and octahedral symmetry and also affects the bond lengths among the lattice sites [24]. However, the  $M_S$  value drastically decreased to about  $45 \text{ emu/cm}^3$  for  $\text{Pr}_2\text{Bi}_1\text{Fe}_5\text{O}_{12}$ , which has the highest Pr content. These results are in good agreement with the FR measurements; the  $\text{Pr}_1\text{Y}_1\text{Bi}_1\text{Fe}_5\text{O}_{12}$  thin film, which had the highest  $M_S$  value, also had the largest  $\theta_{\text{max}}$  value (Fig. 2(b)).

#### 4. Conclusions

The magnetic and MO properties of  $\text{Pr}_x\text{Y}_{2-x}\text{Bi}_1\text{Fe}_5\text{O}_{12}$  ( $x = 0, 0.25, 0.5, 1,$  and  $2$ ) thin films grown on glass substrate using a modified MOD method were investigated. The effect of Pr content on FR angle was studied in detail. The  $\text{Pr}_1\text{Y}_1\text{Bi}_1\text{Fe}_5\text{O}_{12}$  thin film had excellent MO performance, with a large FR angle of  $-13^\circ/\mu\text{m}$ . The enhancement of the FR angle was attributed to two factors: (i) increased spin-orbit interaction strength and (ii) improving crystallinity, magnetic properties by using proper Pr content substitution. The XRD, SEM, and VSM measurements revealed that introducing  $\text{Pr}^{3+}$  into  $\text{Pr}_x\text{Y}_{2-x}\text{Bi}_1\text{Fe}_5\text{O}_{12}$  provided thin films having high crystallinity, good morphology, and strong  $M_S$  enhancement, which explained the FR angle enhancement. These films are good candidates for MO microscopy and MO device applications.

#### Acknowledgments

This work was supported by research fund of Chungnam National University, South Korea.

#### References

- [1] T. Haider, International Journal of Electromagnetics and Applications **7**, 17 (2017).
- [2] A. Kirihara, K. L. Uchida, Y. Kajiwara, M. Ishida, Y. Nakamura, T. Manako, E. Saitoh, and S. Yorozu, Nat. Mater. **11**, 686 (2012).
- [3] G. B. Scott and D. E. Lacklison, IEEE Trans. Magn. **12**, 292 (1976).
- [4] A. Wada, S. Tanaka, and N. Takahashi, IEEE Photo. J. **5**, 6801108 (2013).
- [5] T. Ishibashi, T. Kosaka, M. Naganuma, and T. Nomura, J. Phys. Conf. Ser. **200**, 112002 (2010).
- [6] O. Galstyan, H. Lee, A. Babajanyan, A. Hakhoumian, B. Friedman, and K. Lee, J. Appl. Phys. **117**, 163914 (2015).
- [7] P. Gornert, T. Aichele, A. Lorentz, R. Hergt, and J. Taubert, Phys. Status Solidi **201**, 1398 (2004).
- [8] M. Gomi, T. Tanida, and M. Abe, J. Appl. Phys. **57**, 3888 (1985).
- [9] P. C. Van, S. Surabhi, V. Dongquoc, R. Kuchi, S. G. Yoon, and J. R. Jeong, Appl. Surf. Sci. **435**, 377 (2018).
- [10] H. Hayashi, S. Iwasa, N. J. Vasa, T. Yoshitake, K. Ueda, S. Yokoyama, S. Higuchi, H. Takeshita, and M. Nakahara, Appl. Surf. Sci. **197**, 463 (2002).
- [11] K. Matsumoto, S. Yamamoto, Y. Yamanobe, A. Ueno, K. Yamaguchi, and T. Fujii, Jpn. J. Appl. Phys. **30**, 1696 (1991).
- [12] A. Azevedo, S. Bharthulwar, W. Eppler, and M. Kryder, IEEE Trans. Magn. **30**, 4416 (1994).
- [13] V. Dongquoc, R. Kuchi, P. C. Van, S. G. Yoon, and J. R. Jeong, Curr. Appl. Phys. **18**, 241 (2018).
- [14] V. Dongquoc, R. Kuchi, P. C. Van, S. Surabhi, S. W. Lee, D. S. Kim, and J. R. Jeong, Ceram. Int. **45**, 20758 (2019).
- [15] T. Ishibashi, A. Mizusama, M. Nagai, S. Shimizu, K. Sato, N. Togashi, T. Mogi, M. Houchido, H. Sano, and K. Kuyiyama, J. Appl. Phys. **97**, 013516 (2004).
- [16] T. Ishibashi, T. Yoshida, T. Kobayashi, S. Ikehara, and T. Nishi, J. Appl. Phys. **113**, 17A926 (2013).
- [17] Frederic J. Kahn and P. S. Pershan, Phys. Rev. **186**, 891 (1969).
- [18] G. B. Scott, D. E. Lacklison, H. I. Ralph, and J. L. Page, Phys. Rev. B **12**, 2562 (1975).
- [19] Z. Simsa, H. Le Gall, J. Simsova, J. Kolacek, and Paillier-Malecot, Le, IEEE Trans. Magn. **20**, 1001 (1984).
- [20] G. F. Dionne and G. Allen, J. Appl. Phys. **73**, 6127 (1993).
- [21] C. Leycuras, H. Le Gall, J. M. Desvignes, M. Guillot, and A. Marchand, J. Appl. Phys. **53**, 8181 (1982).
- [22] J. Yang, Y. Xu, and M. Guillot, J. Phys. Condens. Matter **11**, 3299 (1999).
- [23] P. Hansen, C. P. Klages, and K. Witter, J. Appl. Phys. **60**, 721 (1986).
- [24] M. N. Akhtar, M. Yousaf, S. N. Khan, M. S. Nazir, M. Ahmad, and M. A. Khan, Ceram. Int. **43**, 17032 (2017).
- [25] M. G. Kang, V. Dongquoc, S. Surabhi, B. G. Park, and J. R. Jeong, J. Magn. Mater. **482**, 61 (2019).